NASA
Technical Memorandum 101442

AVSCOM
Technical Report 88-C-040



# Vibration Signature Analysis of Multistage Gear Transmission

F.K. Choy, Y.K. Tu,
and M. Savage
*University of Akron*
*Akron, Ohio*

and

D.P. Townsend
*Lewis Research Center*
*Cleveland, Ohio*



Prepared for the
Fifth International Power Transmission and Gearing Conference
sponsored by the American Society of Mechanical Engineers
Chicago, Illinois, April 25-27, 1989

NASA

US ARMY
AVIATION
SYSTEMS COMMAND
AVIATION R&T ACTIVITY

# VIBRATION SIGNATURE ANALYSIS OF MULTISTAGE GEAR TRANSMISSION

F.K. Choy, Y.K. Tu, and M. Savage
Department of Mechanical Engineering
University of Akron
Akron, Ohio 44235

and

D.P. Townsend
National Aeronautics and Space Administration
Lewis Research Center
Cleveland, Ohio 44135

A-1

ABSTRACT

An analysis is presented for multistage multimesh gear transmission systems. The analysis predicts the overall system dynamics and the transmissibility to the gear box or the enclosed structure. The modal synthesis approach of the analysis treats the uncoupled lateral/torsional modal characteristics of each stage or component independently. The vibration signature analysis evaluates the global dynamics coupling in the system. The method synthesizes the interaction of each modal component or stage with the nonlinear gear mesh dynamics and the modal support geometry characteristics. The analysis simulates transient and steady state vibration events to determine the resulting torque variations, speeds, changes, rotor imbalances and support gear box motion excitations. A vibration signature analysis scheme examines the overall dynamic characteristics of the system, and the individual modal component responses. The gear box vibration analysis also examines the spectral characteristics of the support system.

NOMENCLATURE

| | |
|---|---|
| $A_i(t)$ | modal function of the $i^{th}$ mode in x-direction |
| $A_{ti}(t)$ | modal function of the $i^{th}$ mode in $\theta$-direction |
| $B_i(t)$ | modal function of the $i^{th}$ mode in y-direction |
| $[C_{xx}],[C_{xy}]$ $[C_{yx}],[C_{yy}]$ | bearing direct and cross-coupling damping matrices |
| $[C_t]$ | torsional damping matrix |
| $F_x(t),F_y(t)$ | external excitation forces |
| $F_t(t)$ | external excited moment |
| $F_{Gx}(t),F_{Gy}(t)$ | gear mesh force in x- and y-directions |
| $F_{GT}(t)$ | gear mesh torque |
| $[I]$ | identity matrix |
| $[J]$ | rotational (mass moment of inertia) matrix |
| $K_{KtiK}$ | gear mesh stiffness between $i^{th}$ and $k^{th}$ rotor |
| $[K_s]$ | shaft stiffness matrix |
| $[K_{xx}],[C_{xy}]$ $[K_{yx}],[K_{yy}]$ | bearing direct and cross-coupling stiffness matrix |
| $[M]$ | mass-inertia matrix |
| $R_{ci}$ | radius of gear in the $i^{th}$ rotor |
| $T_F$ | gear generated torque |
| $X_F,Y_F$ | gear forces in x- and y-directions |
| $x_{ci},y_{ci}$ | gear displacements in x- and y-directions of the $i^{th}$ rotor |
| $\alpha_{Ki}$ | angle of tooth mesh between $k^{th}$ and $i^{th}$ rotor |
| $[\lambda^2],[\lambda_t^2]$ | lateral and torsional eigenvalue diagonal matrices |
| $[\phi]_K,[\phi_t]_K$ | lateral and torsional orthonormal eigenvector matrices of the $k^{th}$ rotor |

## INTRODUCTION

The art and science of analyzing gear transmission systems continue to improve. Power transfer is necessary from source to application in mechanical systems. Today's engineers and researchers now delve into areas of innovative advancement. They seek to quantify, establish, and codify methods which can make gear systems meet the ever-widening needs of advancing technology. Their objectives are basic improvements in transmission life, efficiency, maintainability, and reliability. They also seek to reduce noise, weight and

vibration during transmission operation. Gear transmission system studies have included two main efforts. These studies have been on: (1) the localized tooth stress/thermal effects during gear interactions, and (2) the overall global dynamic behavior of the systems.

The objective of this paper is to analyze the overall global dynamics of multistage gear systems using localized gear stress/displacement relationships. Equations of motion are developed for each gear stage in both lateral and torsional directions. Gear mesh force and moment relationships couple the lateral and torsional vibrations and the dynamics of each gear stage. Orthonormal modes of the system transform the equations of motion to modal coordinates. A self-adaptive variable time stepping integration scheme calculates the transient dynamics of the system (Choy, 1988). A typical three-stage multimesh gear system serves as an example. The results of the global dynamics of the system are examined in both time and frequency domains using a FFT (Fast Fourier Transform) procedure (Choy, 1987 and 1988).

## DEVELOPMENT OF EQUATIONS OF MOTION

For a single stage multimass gear-rotor-bearing system, the equations of motion in the X-Z plane in matrix form (Choy, 1987; David, 1987 and 1988) are:

$$[M]\{\ddot{x}\} + [C_{xx}]\{\dot{x}\} + [C_{xy}]\{\dot{y}\} + [K_{xx} + K_s]\{x\} + [K_{xy}]\{y\} = \{F_x(t)\} + \{F_{Gx}(t)\} \quad (1)$$

In the Y-Z plane, the equations are:

$$[M]\{\ddot{y}\} + [C_{yx}]\{\dot{x}\} + [C_{yy}]\{\dot{y}\} + [K_{yy} + K_s]\{y\} + [K_{yx}]\{x\} = \{F_y(t)\} + \{F_{Gy}(t)\} \quad (2)$$

Here $F_x$ and $F_y$ are force excitations from the effects of imbalance, shaft bow and support base motion. $F_{Gx}$ and $F_{Gy}$ are forces induced from the gear mesh interaction with other stages.

The torsional equation of motion of the single stage system is:

$$[J]\{\ddot{\theta}\} + [C_T]\{\dot{\theta}\} + [K_T]\{\theta\} = \{F_T(t)\} + \{F_{Gt}(t)\} \quad (3)$$

In Eq. 3, $F_t$ represents the externally induced torque and $F_{Gt}$ represents the gear mesh induced moment. Note that Eqs. 1 to 3 repeat for each gear stage. The gear mesh forces couple the force equations for each stage to each other and the torsional equations to the lateral equations (David, 1987; Lin, 1988; Mitchell, 1983). Torsional, lateral and interstage coupling relationships appear in the next section.

## COUPLING IN GEAR MESHES

Gear mesh forces and moments are functions of the relative motion and rotation between the two meshing gears and the corresponding gear mesh stiffnesses. These stiffnesses vary in a repeating nonlinear pattern (Cornell, 1981; Pike, 1987; Savage, 1986). The pattern repeats with every tooth pair engagement and acts as a source of excitation at each mesh. Figure 1 shows the coordinate system for the following force and moment equations. Summing the forces, which act on the $K^{th}$ stage of the system, in the X-direction results in:

$$X_F = \sum_{\substack{i=1 \\ i\neq K}}^{n} K_{tKi}\left[-R_{ci}\theta_{ci} - R_{cK}\theta_{cK} + (x_{ci} - x_{cK})\cos\alpha_{Ki} + (y_{ci} - y_{cK})\sin\alpha_{Ki}\right]\cos\alpha_{Ki} \quad (4)$$

Summing the forces in the Y-direction results in:

$$X_F = \sum_{\substack{i=1 \\ i\neq K}}^{n} K_{tKi}\left[-R_{ci}\theta_{ci} - R_{cK}\theta_{cK} + (x_{ci} - x_{cK})\cos\alpha_{Ki} + (y_{ci} - y_{cK})\sin\alpha_{Ki}\right]\sin\alpha_{Ki} \quad (5)$$

Summing moment in the Z-direction results in:

$$T_F = \sum_{\substack{i=1 \\ i\neq K}}^{n} R_{cK}\left[K_{tKi}(-R_{ci}\theta_{ci} - R_{cK}\theta_{cK})\right] \quad (6)$$

where n is the number of stages in the system.

## MODAL ANALYSIS

To reduce the computational effort, the number of degrees-of-freedom of the system is reduced through modal transformation. Orthonormal modes for each stage result from solving the system homogeneous characteristic equations. For lateral modes, the equations are:

$$[M]\{\ddot{x}\} + \left[K_s + \frac{K_{xx} + K_{yy}}{2}\right]\{x\} = 0 \quad (7)$$

For torsional modes, the equations are:

$$[J]\{\ddot{\theta}\} + [K_T]\{\theta\} = 0 \quad (8)$$

Averaged X- and Y-direction support stiffnesses bring the calculated mode shapes closer to reality. Using the modal expansion theorem yields (Choy, 1987):

$$\{x\} = \sum_{i=1}^{m} A_i\{\phi_i\} \quad (9)$$

$$\{y\} = \sum_{i=1}^{m} B_i\{\phi_i\} \quad (10)$$

$$\{\theta\} = \sum_{i=1}^{m} A_{ti}\{\phi_{ti}\} \quad (11)$$

where m is the number of modes used. With the following orthogonality conditions,

$$[\phi]^T[K][\phi] = [\lambda^2] \tag{12}$$

$$\left[\phi_t\right]^T\left[K_t\right]\left[\phi_t\right] = \left[\lambda_t^2\right]$$

$$[\phi]^T[M][\phi] = \left[\phi_t\right]^T[J]\left[\phi_t\right] = [I] \tag{13}$$

the equations of motion in modal coordinates become:

$$\{\ddot{A}\} + [\phi]^T\left[C_{xx}\right][\phi]\{\dot{A}\} + [\phi]^T\left[C_{xy}\right][\phi]\{\dot{B}\} + \left[\lambda^2\right]\{A\}$$
$$+ [\phi]^T\left[K_{xy}\right][\phi]\{B\} = [\phi]^T\{F_x(t) + F_{Gx}(t)\} \tag{14}$$

$$\{\ddot{B}\} + [\phi]^T\left[C_{yy}\right][\phi]\{\dot{B}\} + [\phi]^T\left[C_{yx}\right][\phi]\{\dot{A}\} + \left[\lambda^2\right]\{B\}$$
$$+ [\phi]^T\left[K_{yx}\right][\phi]\{A\} = [\phi]^T\{F_y(t) + F_{Gy}(t)\} \tag{15}$$

$$\{\ddot{A}_t\} + \left[\phi_t\right]^T\left[C_T\right]\left[\phi_t\right]\{\dot{A}_t\} + \left[\lambda_t^2\right]\{A_t\}$$
$$= \left[\phi_t\right]^T\{F_t(t) + F_{Gt}(t)\} \tag{16}$$

Thus, the gear mesh force and moment coupling equations for the $K^{th}$ stage in the modal form are:

$$[\phi]_K^T\{X_F\} = \sum_{j=1}^{m}\phi_{Kj\ell}\left\{\sum_{\substack{i=1\\ i\neq K}}^{n} K_{tKi}\left[-R_{ci}\theta_{ci} - R_{cK}\theta_{cK}\right.\right.$$
$$\left.\left. + \left(x_{ci} - x_{cK}\right)\cos\alpha_{Ki} + \left(y_{ci} - y_{cK}\right)\sin\alpha_{Ki}\right]\cos\alpha_{Ki}\right\} \tag{17}$$

$$[\phi]_K^T\{Y_F\} = \sum_{j=1}^{m}\phi_{Kj\ell}\left\{\sum_{\substack{i=1\\ i\neq K}}^{n} K_{tKi}\left[-R_{ci}\theta_{ci} - R_{cK}\theta_{cK}\right.\right.$$
$$\left.\left. + \left(x_{ci} - x_{cK}\right)\cos\alpha_{Ki} + \left(y_{ci} - y_{cK}\right)\sin\alpha_{Ki}\right]\sin\alpha_{Ki}\right\} \tag{18}$$

$$[\phi]_K^T\{T_F\} = \sum_{j=1}^{m}\phi_{Kj\ell}\left\{\sum_{\substack{i=1\\ i\neq K}}^{n} R_{cK}\left[K_{tKi}\left(-R_{ci}\theta_{ci}\right.\right.\right.$$
$$\left.\left.\left. - R_{cK}\theta_{cK}\right)\right]\right\} \tag{19}$$

where $\ell$ is the station location of the gear in the $K^{th}$ stage (Boyd, 1987; August, 1986).

SOLUTION PROCEDURE

Rearrange the modal equations of motion developed in Eqs. (14) to (16) into:

X-equation

$$\{\ddot{A}\} = -[\phi]^T\left[C_{xx}\right][\phi]\{\dot{A}\} - [\phi]^T\left[C_{xy}\right][\phi]\{\dot{B}\} - \left[\lambda^2\right]\{A\}$$
$$- [\phi]^T\left[K_{xy}\right][\phi]\{B\} + [\phi]^T\{F_x(t) + F_{Gx}(t)\} \tag{20}$$

Y-equation

$$\{\ddot{B}\} = -[\phi]^T\left[C_{yy}\right][\phi]\{\dot{B}\} - [\phi]^T\left[C_{yx}\right][\phi]\{\dot{A}\} - \left[\lambda^2\right]\{B\}$$
$$- [\phi]^T\left[K_{yx}\right][\phi]\{A\} + [\phi]^T\{F_y(t) + F_{Gy}(t)\} \tag{21}$$

and, Θ-equation;

$$\{\ddot{A}_t\} = -\left[\phi_t\right]^T\left[C_T\right]\left[\phi_t\right]\{\dot{A}_t\} - \left[\lambda_t^2\right]\{A_t\}$$
$$+ \left[\phi_t\right]^T\{F_t(t) + F_{Gt}(t)\} \tag{22}$$

A variable time stepping Newmark-Beta integration scheme evaluates the modal velocity and displacement at each time interval. In turn, Eqs. 9 through 11 transform the modal displacements into absolute/relative displacements in fixed coordinates.

DISCUSSION OF RESULTS

To demonstrate the application of the analytical method, a three-stage multimesh gear system serves as an example. Figure 2 shows the geometry of the gear system. Stage 1 is the driver stage. The stage 1 gear drives both the output gears directly at a speed of 1500 rpm. Its input torque of 2.25 kN-m is split equally between the two output stages. All the meshes are identical with 36 teeth and a contact ratio of 1.6 as shown in Fig. 3. Although similar, the lateral support stiffness for stage 2 is greater than that for

stage 3. The system has only minimal imbalances to make the torsional vibration of the system more pronounced than the lateral. Figure 4 shows the lateral vibration orbits for all three stages at the mesh locations. Note that the difference in orbit sizes result from the differences in imbalance and shaft stiffness for each stage. While stages 2 and 3 maintain a relative circular orbit, stage 1 exhibits an elliptical motion due to the tooth mesh stiffness interactions with stages 2 and 3.

Figures 5 and 6 show the gear mesh forces in both time and frequency domains between stages 1-2 and 3-4. A substantially larger force is present in the 1-3 mesh than in the 1-2 mesh. This is mainly due to the fact that stage 3 possesses higher vibrational magnitude than stage 2. The orbit sizes shown in Fig. 4 illustrate this difference. Stage 3's support stiffness is less than that of stage 2.

Table 1 lists both the undamped lateral and torsional natural frequencies of all three stages with their corresponding bearing supports. Figure 6 shows that the dominating components at stage 1-2 are the tooth mesh frequency of 900 Hz and the first stage torsional natural frequency of 355 Hz. A large average force component at zero frequency is also present. But this component does not contribute to the transmission vibrations. A considerable force also occurs at the input shaft rotational frequency of 25 Hz while a smaller component is present in the stage 2 torsional mode at 880 Hz. A small force echo is also present in stage 2 at the stage 3 torsional natural frequency of 280 Hz. Similar observations are possible with the stage 1-3 force frequency diagram.

Figure 7 and 8 show the first three modal contributions of stage 1 in both the time and frequency domains. The corresponding mode shapes are in Fig. 9. Figure 7 shows both fixed (d.c.) and varying (a.c.) responses in each mode. The response magnitude decreases with increasing mode number. The frequency domain plot of Fig. 8 shows all the modes excited at their own natural frequencies. The ratio of fixed (d.c.) to varying (a.c.) signal magnitudes in Fig. 8 decreases as the mode number increase. Figures 10, 11 and 12 are plots of the time response, frequency response and mode shapes for the first lateral mode of each stage. These figures provide the modal information of the lateral vibration of all three stages. Note that the rotational frequency of 25 Hz is excited in all three stages. Figure 11 shows that stage 3, the first lateral frequency of 115 Hz is also excited. This is due to the characteristic of its mode shape which is shown in Fig. 12.

## CONCLUSIONS

This paper presents a vibration signature analysis for multistage gear transmissions. The analysis combines gear mesh dynamics and structural modal analysis to study the transmission vibrations. This is a comprehensive method of analyzing multistage gear system with effects of geometry complexity, support flexibility, mass imbalance and shaft bow. In this method:

1. The modal method transforms the equations of motion into modal coordinates to reduce the degrees-of-freedom of the system;

2. Gear force observations in both the time and frequency domains provide good insights into the source of dominating response forces;

3. Knowledge of modal excitations provide an understanding of the vibrational characteristics of the system which can result in improved transmission performance and durability; and

4. The coupling effects of connected structures such as the gearbox are easily included in the existing modal analysis without sacrificing the above advantages.

## REFERENCES


August, R. and Kasuba, R., 1986, "Torsional Vibrations and Dynamic Loads in a Basic Planetary Gear System," Journal of Vibration, Acoustics, Stress, and Reliability in Design, Vol. 108, No. 3, pp. 348-353.

Boyd, L.S. and Pike, J., 1987, "Epicyclic Gear Dynamics," AIAA Paper 87-2042.

Choy, F.K. and Li, W.H., 1987, "Frequency Component and Modal Synthesis Analysis of Large Rotor-Bearing Systems with Base Motion Induced Excitations," Journal of the Franklin Institute, Vol. 323, No. 2, pp. 145-168.

Choy, F.K., Padovan, J., and Li, W.H., 1988, "Rub in High Performance Turbomachinery, Modeling, Solution Methodology, and Signature Analysis," Mechanical Systems and Signal Processing, Vol. 2, No. 2, pp. 113-133.

Choy, F.K., Townsend, D.P., and Oswald, F.B., 1988, "Dynamic Analysis of Multimesh-Gear Helicopter Transmissions," NASA TP-2789.

Cornell, R.W., 1981, "Compliance and Stress Sensitivity of Spur Gear Teeth," Journal of Mechanical Design, Vol. 103, No. 2, pp. 447-459.

David, J.W., Mitchell, L.D., and Daws, J.W., 1987, "Using Transfer Matrices for Parametric System Forced Response," Journal of Vibration, Acoustics, Stress, and Reliability in Design, Vol. 109, No. 4, pp. 356-360.

David, J.W. and Park, N., 1987, "The Vibration Problem In Gear Coupled Rotor Systems," Rotating Machinery Dynamics, Vol. 2, A. Muszynska and J.C. Simmons, eds., ASME, New York, 1987, pp. 297-303.

Lin, H., Huston, R.L., and Coy, J.J., 1988, "On Dynamic Loads in Parallel Shaft Transmissions: Part I - Modelling and Analysis," Journal of Mechanisms, Transmissions and Automation in Design, Vol. 110, No. 2, pp. 221-226.

Mitchell, L.D. and David, J.W., 1985, "Proposed Solution Methodology for the Dynamically Coupled Nonlinear Geared Rotor Mechanics Equations," Journal of Vibration, Acoustics, Stress, and Reliability in Design, Vol. 107.

Savage, M., Caldwell, R.J., Wisor, G.D., and Lewiciki, D.G., 1986, "Gear Mesh Compliance Modeling," NASA TM-88843.

TABLE I. - SYSTEM NATURAL FREQUENCIES

| Mode | Stage 1 | Stage 2 | Stage 3 |
|---|---|---|---|
| Torsion natural frequencies, Hz | | | |
| 1 | 355 | 550 | 280 |
| 2 | 1090 | 1610 | 820 |
| Lateral natural frequencies, Hz | | | |
| 1 | 115 | 160 | 110 |
| 2 | 145 | 189 | 200 |
| 3 | 190 | 264 | 260 |

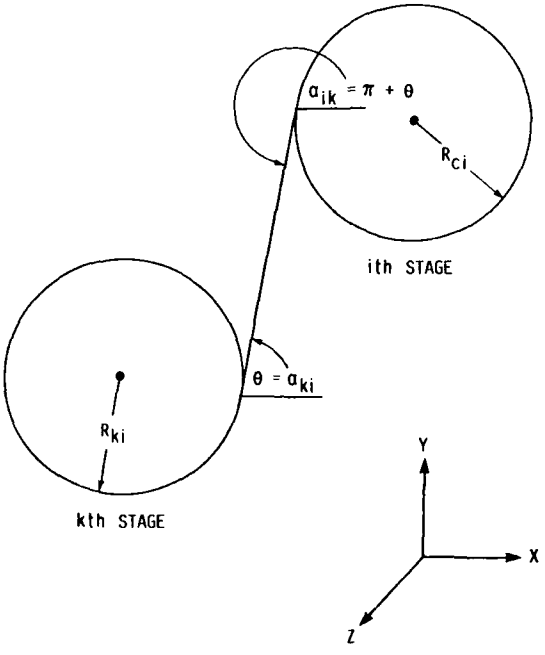


FIGURE 1. - COORDINATE SYSTEM FOR GEAR MESH FORCE AND MOMENT.

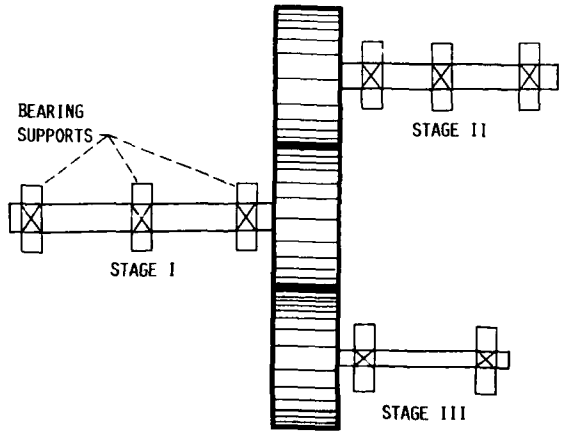


FIGURE 2. - TYPICAL THREE STAGE ROTOR-BEARING-GEAR SYSTEM.

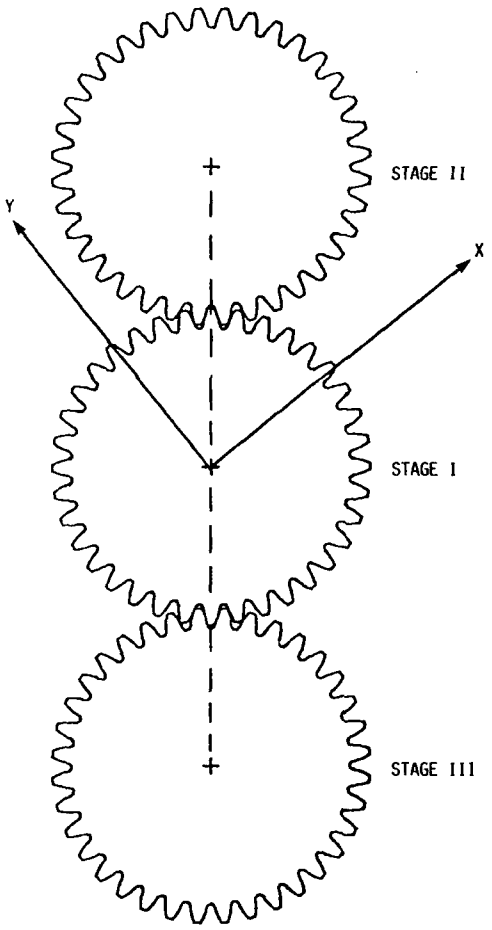


FIGURE 3. - GEAR MESH SYSTEM USED AS EXAMPLE.

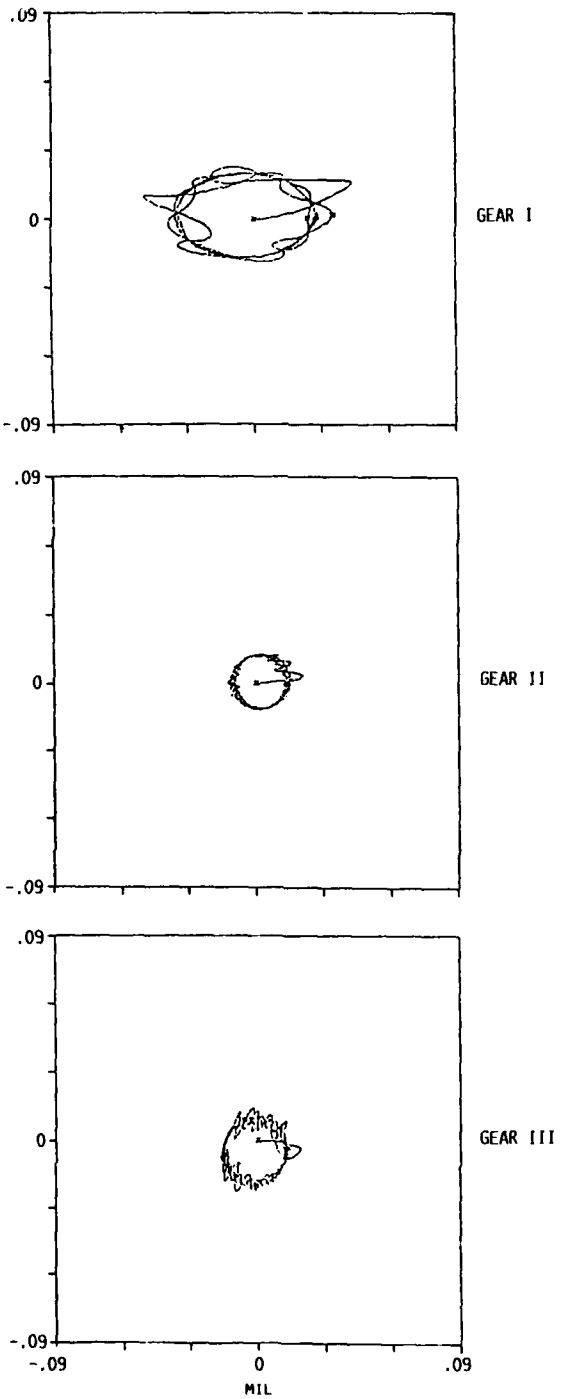


FIGURE 4. - ROTOR ORBITS AT THE GEAR LOCATIONS FOR ALL THREE STAGES.

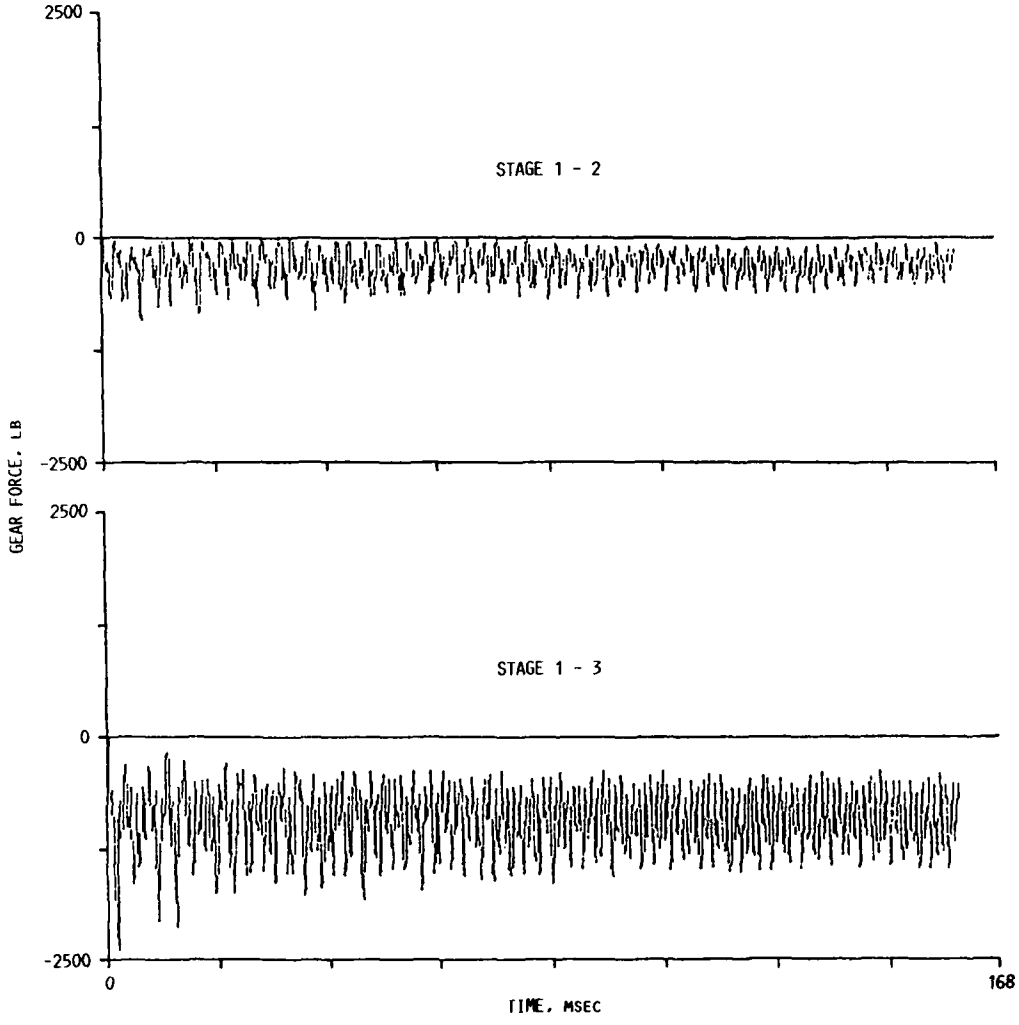


FIGURE 5. - GEAR FORCES IN TIME DOMAIN.

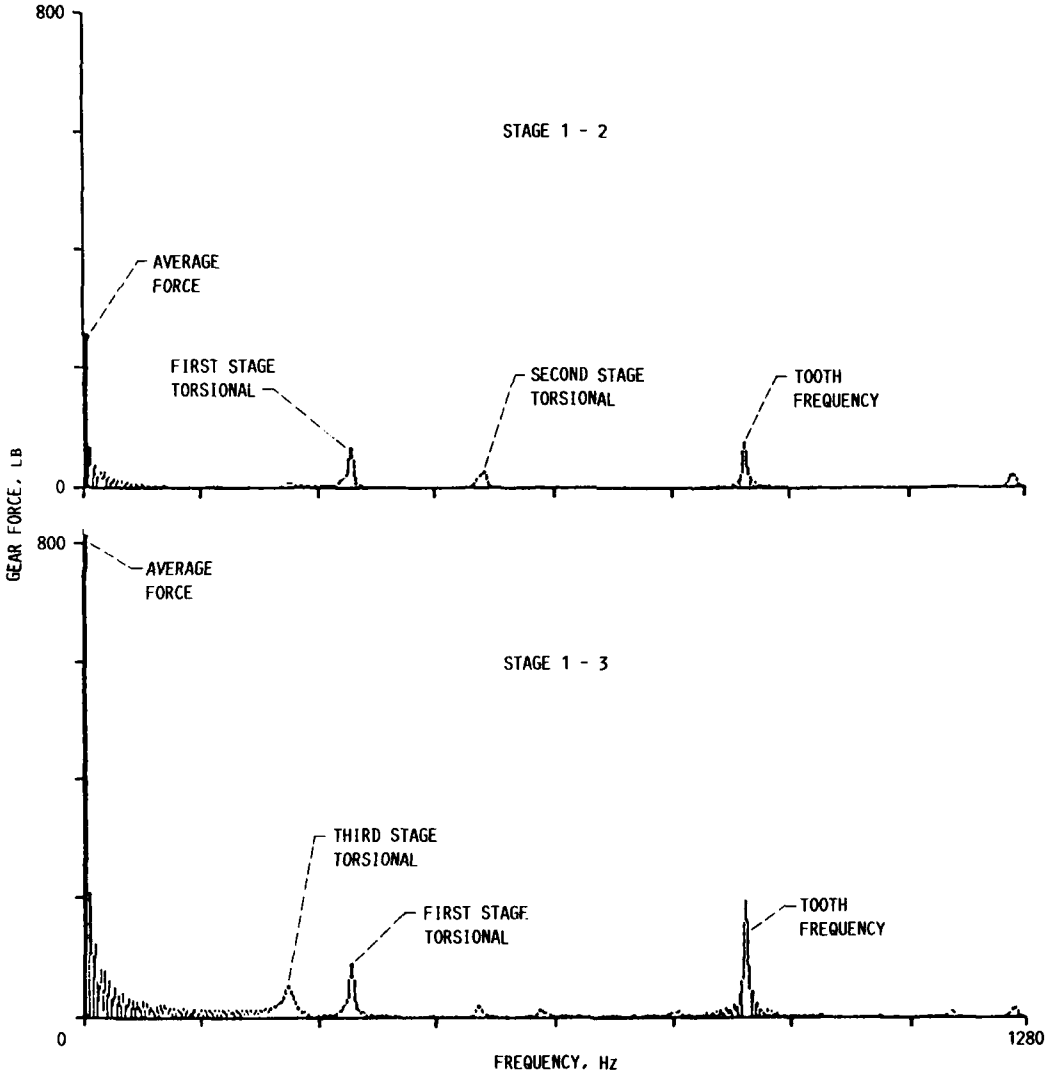


FIGURE 6. - GEAR FORCES IN FREQUENCY DOMAIN.

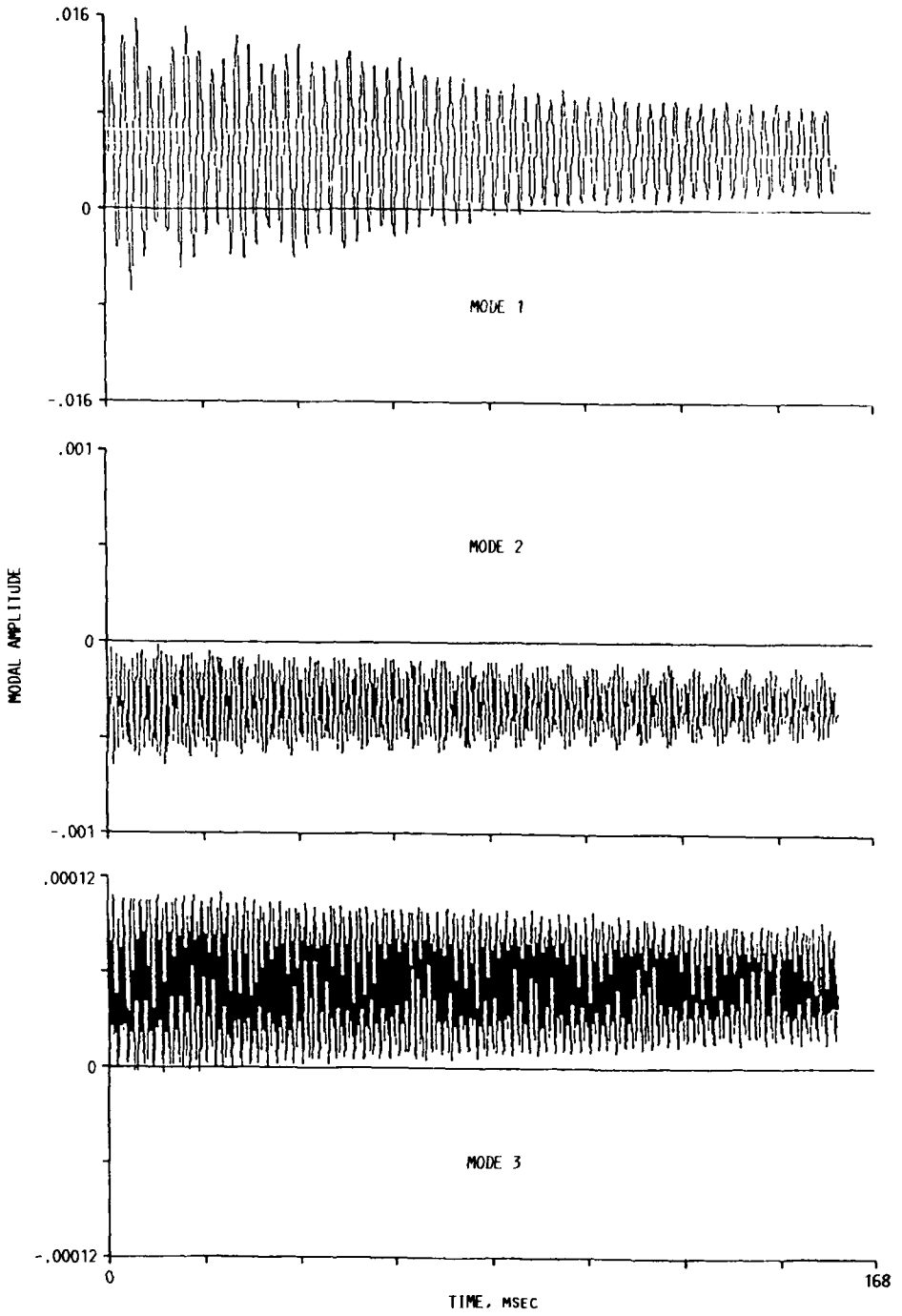


FIGURE 7. - FIRST STAGE TORSIONAL MODAL EXCITATIONS IN TIME DOMAIN.

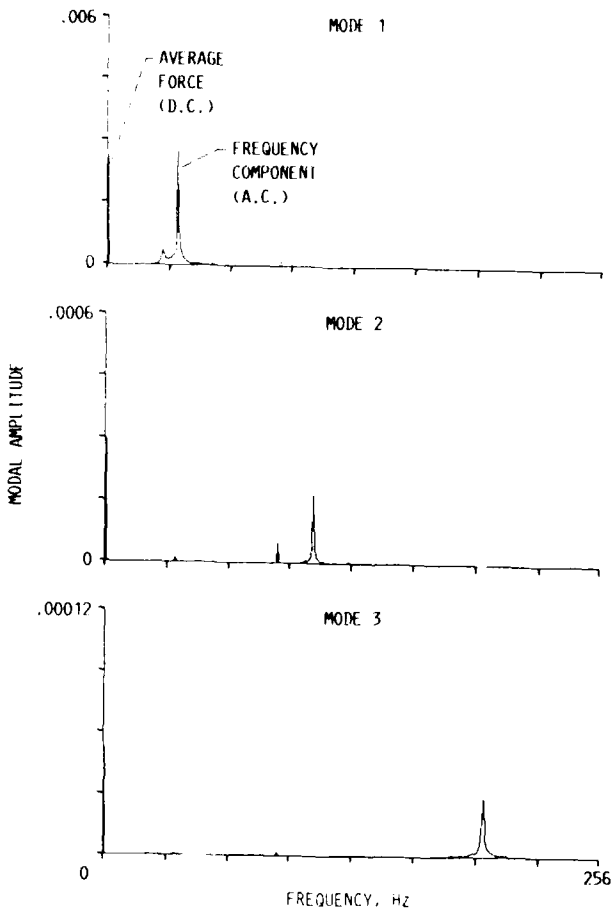


FIGURE 8. - FIRST STAGE TORSIONAL MODAL EXCITATIONS IN FREQUENCY DOMAIN.

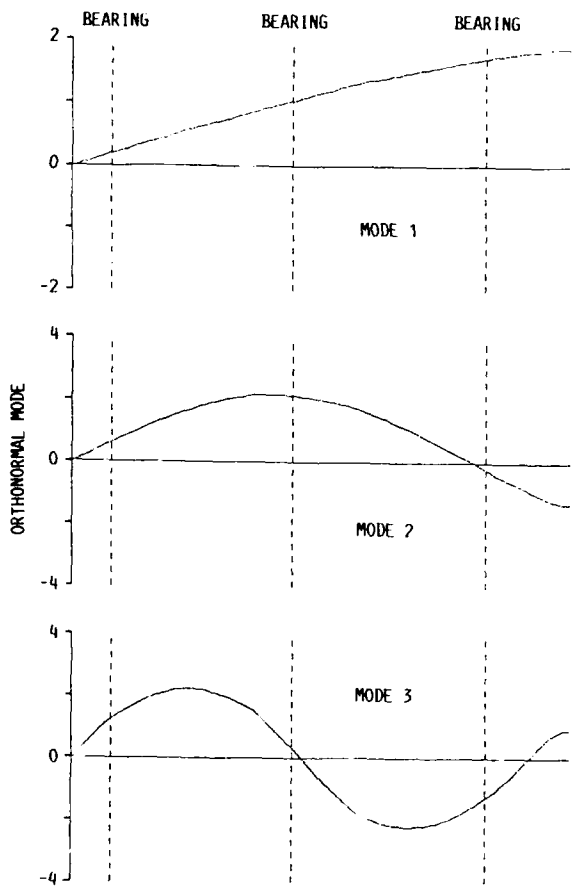


FIGURE 9. - FIRST STAGE NORMALIZED TORSIONAL MODES.

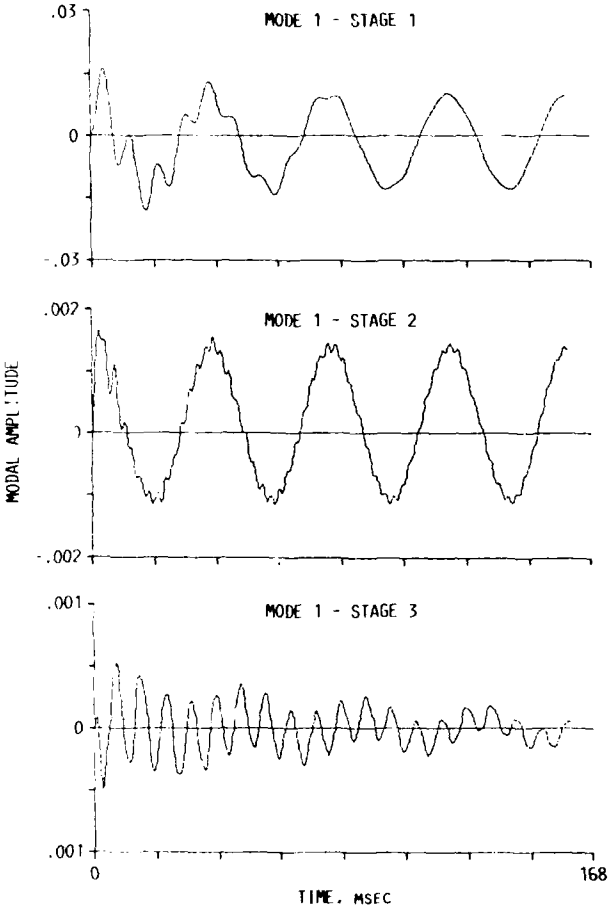


FIGURE 10. - FIRST LATERAL MODE EXCITATION IN TIME DOMAIN.

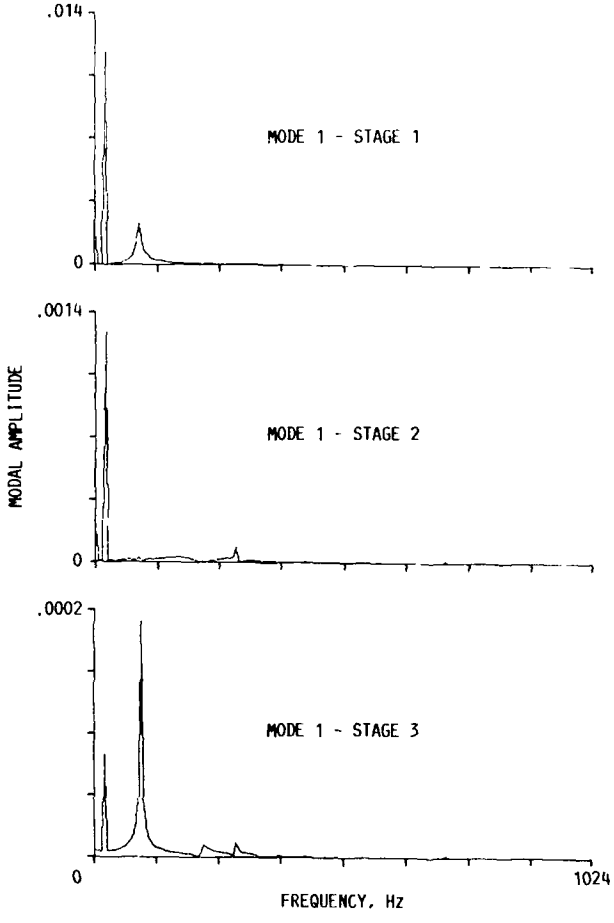


FIGURE 11. - FIRST LATERAL MODE EXCITATION IN FREQUENCY DOMAIN.

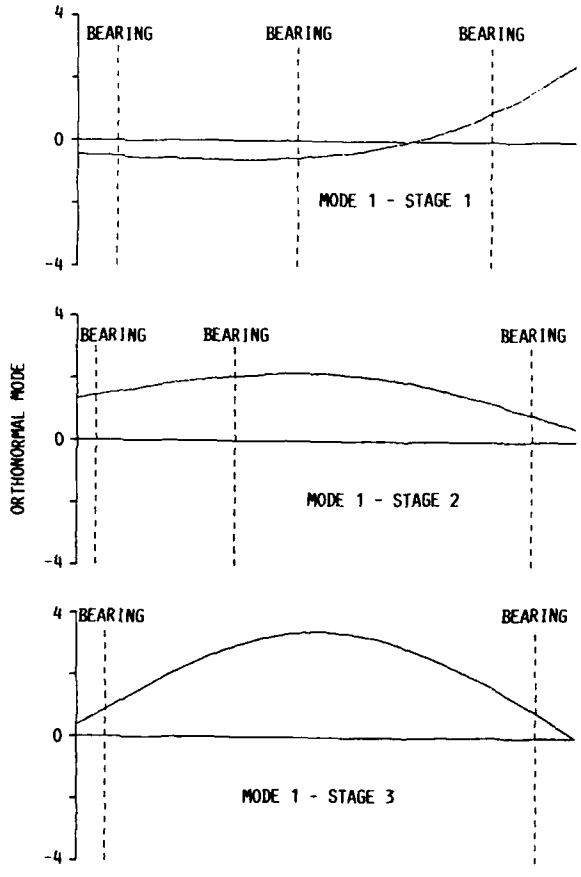


FIGURE 12. - ORTHONORMAL MODE SHAPE FOR THE FIRST LATERAL MODE.